Available online at www.sciencedirect.com
ScienceDirect
International Journal of Coal Geology 70 (2007) 166–183
International Journal of COAL GEOLOGY
www.elsevier.com/locate/ijcoalgeo

Quantitative evaluation of minerals in coal deposits in the Witbank and Highveld Coalfields, and the potential impact on acid mine drainage

K.L. Pinetown [a,*], Colin R. Ward [b], W.A. van der Westhuizen [c]

[a] CSIRO Petroleum, P. O. Box 136, North Ryde, NSW, 1670, Australia
[b] School of Biological, Earth and Environmental Sciences, University of New South Wales, Sydney, 2052, Australia
[c] Department of Geology, University of the Free State, P. O. Box 339, Bloemfontein, 9300, South Africa

Received 14 February 2005; accepted 21 February 2006
Available online 2 August 2006

Abstract

This study has investigated the quantitative distribution of minerals in coals and other lithological units in the coal-bearing successions of the Witbank and Highveld Coalfields in the Mpumalanga Province of South Africa, using low-temperature oxygen-plasma ashing (LTA), high temperature ashing, X-ray diffraction, and X-ray fluorescence spectrometry techniques. Mineral matter makes up approximately 8 to 35 wt.% of the coal samples. SiO_2 concentrations in the coal vary between 0.0 and 35.0 wt.%, Al_2O_3 between 0.5 and 16.0 wt.%, Fe_2O_3 between 0.03 and 10.0 wt.%, and S between 0.15 and 8.0 wt.%. Minor concentrations of CaO (0.0 to 8.0 wt.%) and MgO (0.0 to 1.0 wt.%) are also present. P_2O_5 occurs in concentrations of 0.0 to 3.5 wt.% and K_2O is in the order of 0.0 to 1.3 wt.%. Na_2O varies between 0.0 and 0.45 wt.%, with the Highveld coals showing an enrichment in Na_2O (0.0 to 0.51 wt.%) in comparison with the Witbank coals. The minerals in the coals are dominated by quartz and kaolinite, with varying proportions of calcite, dolomite and pyrite, as well as accessory phosphate phases. Higher (normalised) K_2O and Na_2O concentrations are present in the sandstones than in the associated siltstones and carbonaceous shales, partly reflecting the presence of feldspars and clay minerals such as illite.

Acid–base accounting was used to investigate the potential of the coal and coal-bearing units to produce acid mine drainage conditions. According to the screening criteria, all the coal and coal-bearing units, except the unit between the No. 1 and No. 2 coal seams, are potentially acid generating. The average Net Neutralising Potential (NNP) values suggest that the No. 5 coal seam, the No. 4 Upper coal seam, and the unit between the No. 4 and No. 2 coal seams are potentially acid generating. With such techniques it is possible to predict the types of situations that might arise concerning groundwater quality, and implement proper prevention or remediation programs.
© 2006 Elsevier B.V. All rights reserved.

Keywords: Coal mineralogy; Low-temperature ashing; X-ray diffraction; X-ray fluorescence; Acid mine drainage

1. Introduction

Acid mine drainage (AMD) conditions are primarily caused by the oxidation of sulphide minerals and migration of the oxidation products into solution. In coal mines the minerals pyrite and marcasite (FeS_2) are

* Corresponding author. Fax: +27 17 614 5176.
E-mail address: kaydyp@bigpond.net.au (K.L. Pinetown).

0166-5162/$ - see front matter © 2006 Elsevier B.V. All rights reserved.
doi:10.1016/j.coal.2006.02.013

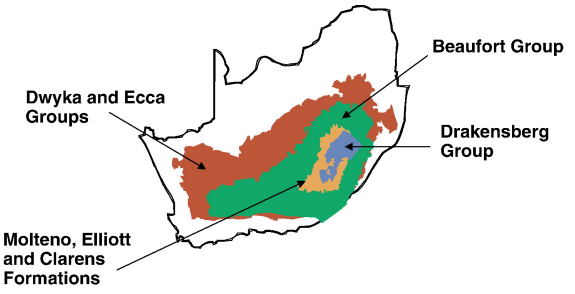

Fig. 1. Outcrop of Karoo Supergroup units within the Karoo Basin.

largely responsible for any AMD problems. The use of water during coal mining, in conjunction with atmospheric exposure, provides a suitable medium to supply sufficient oxygen for pyrite oxidation to occur. Waters affected by these reactions are often strongly acidic, and may build up in significant quantities in underground workings and aquifers.

Various reactions between these waters and many other mineral phases may give rise to a complex combination of dissolved constituents, with numerous adverse effects on the surrounding environment. Interactions between minerals and the immediate environment, especially the surrounding groundwater, may create significant environmental problems associated with coal mining. In order to specify the cause and find a solution to any such problems it is necessary to investigate the nature of the coal (i.e. the minerals and macerals present), and attempt to quantify the extent to which interaction has taken place or could take place between the coal or coal-bearing strata and the surrounding environment.

The mineral matter in coals and other sediments provides significant information on the depositional conditions and geological history of the coal-bearing sequences and individual coal beds. Individual coal samples may contain similar assemblages of major and minor minerals, but there may also be differences in the relative abundance, and possibly also in the modes of occurrence and the genesis of these particular minerals. Discussions of different aspects of the mineral matter in coal are given by authors such as Williamson (1967), Mackowsky (1968), Bouška (1981), Ward (1984, 1986), Spiker et al. (1994), McCarthy et al. (1998), Rao and Walsh (1999), Ward et al. (1999, 2001a,b), Vassilev and Tascon (2002), and Ward (2002), but for various reasons there is little discussion in the international literature on the mineral matter in South African coal deposits.

The mineral matter in South African coals is dominated by clay minerals, mainly kaolinite and illite, followed by quartz and then the carbonates calcite, dolomite and siderite (Gaigher, 1980). Pyrite may also be present, however, and even represent an abundant component of the mineral matter in some instances. The

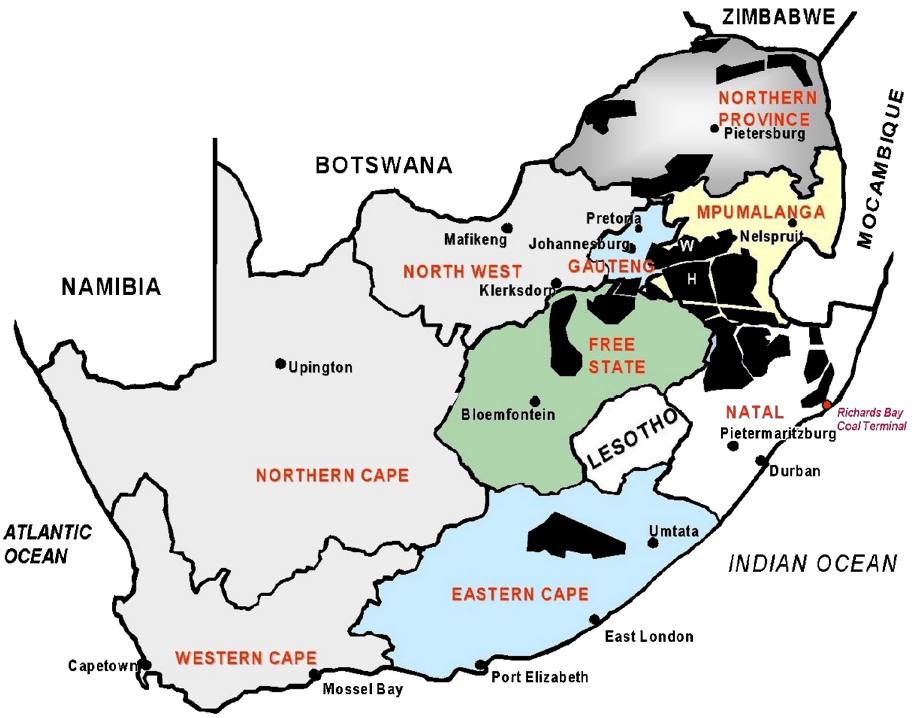

Fig. 2. The distribution of the South African coalfields and locality map of the Witbank and Highveld Coalfields.

main objective of the present study was to provide a more comprehensive mineralogical database for coals and associated strata in the Witbank and Highveld Coalfields, both to improve the understanding of coal characterisation and to relate the mineralogy of the different materials to their potential for producing acidic or alkaline mine waters associated with mining and preparation processes.

2. Geological setting

The main coal deposits of South Africa occur in the Karoo Basin, which is a retro-arc foreland basin developed in front of the Cape Fold Belt in association with the Late Palaeozoic–Early Mesozoic subduction of the palaeo-Pacific Plate beneath the Gondwana Plate. The maximum thickness of the Karoo sedimentary succession (Karoo Supergroup) exceeds 6 km, and the sediments reflect environments ranging from glacial to deep marine, deltaic, fluvial and aeolian (Catuneanu et al., 1998). A period of glacial sedimentation marked the beginning of Karoo Supergroup deposition, and gave rise to deposition of the Dwyka Group. After glaciation a shallow sea remained (Smith et al., 1993), and black clays and mud accumulated on the submerged platform under cold climatic conditions to form the Lower Ecca Group, over which deltas prograded and eventually combined to form broad alluvial plains constituting the Upper Ecca Group (Smith and Whittaker, 1986a). Towards the end of the Late Permian the deposits of the Beaufort Group formed on semi-arid alluvial plains, mainly as a result of floodplain aggradation. Debris fans prograded into the central parts of the basin (Molteno Formation), and these fans were later drained by meandering river systems (Elliot Formation). Sediments formed by the periodic river floods, together with aeolian sand dune deposits, were preserved as the Clarens Formation. Volcanic flows of the Drakensberg Group, overlying this sequence, mark the end of the Karoo Supergroup formation (Fig. 1).

The Witbank Coalfield is situated east of Johannesburg (Fig. 2), and the Highveld Coalfield is situated south of the Witbank Coalfield. The fields are characterised by numerous post-Karoo age dolerite sills and dykes, and rocks of the Vryheid Formation of the Ecca Group cover most of the area. Five separate bituminous coal seams are preserved in the Vryheid Formation, deposited under cool, wet climatic conditions. The strata of the Vryheid Formation and the Dwyka Group, which form the main part of the Karoo Supergroup in the study area, consist primarily of sandstone, carbonaceous shale, siltstone and minor conglomerate (Cairncross, 2001). The sediments were deposited on an undulating floor, which influenced the distribution and thickness of the sedimentary successions as well as the quality of coal seams (Smith and Whittaker, 1986b).

The distribution of the coal seams is controlled by the pre-Karoo topography, but the coals are mainly flat-lying or dip only slightly in a southerly direction. Steeper dips are encountered in the lower seams, while seams Nos. 4 and 5 have a rather regular disposition. The strata of the Karoo are generally undeformed, but have abundant small faults. Dolerite dykes and sills have affected most of the areas of the coalfields. Large

Table 1
Information on sample set used for experiments

Sample	Stratigraphy	Location	Sample type	Rock type
BH 1-5	No. 4 lower	Highveld Coalfield	Borehole core	Coal
DOU-37	No. 2 lower	Witbank Coalfield	Seam sub-section	Coal
KHU 10-2	No. 2	Witbank Coalfield	Grab sample	Coal
KOR-10	No. 2	Witbank Coalfield	Grab sample	Coal
LK-1	No. 2	Witbank Coalfield	Grab sample	Coal
LU-13	No. 2	Witbank Coalfield	Grab sample	Coal
M-20	No. 4	Witbank Coalfield	Grab sample	Coal
OPT-12	No. 2 lower	Witbank Coalfield	Grab sample	Coal
R2-M	No. 2	Witbank Coalfield	Grab sample	Coal
DEL-4	No. 4	Witbank Coalfield	Seam sub-section	Coal
LU-1	No. 2	Witbank Coalfield	Grab sample	Coal
LU-24	No. 2	Witbank Coalfield	Grab sample	Coal
BHW 1-3	No. 4 lower roof	Highveld Coalfield	Borehole core	Sandstone
DOU-35	No. 2 roof	Witbank Coalfield	Seam sub-section	Siltstone
DOU-39	No. 2 floor	Witbank Coalfield	Seam sub-section	Sandstone
M-21	No. 4 floor	Witbank Coalfield	Grab sample	Siltstone
M-22	No. 4 floor	Witbank Coalfield	Grab sample	Sandstone
OPT-3	No. 4 parting	Witbank Coalfield	Grab sample	Sandstone
OPT-11	No. 2 parting	Witbank Coalfield	Grab sample	Sandstone
R2RO	No. 2 roof	Witbank Coalfield	Grab sample	Siltstone
R4FLG	No. 4 floor	Witbank Coalfield	Grab sample	Sandstone
R4PT	No. 4 parting	Witbank Coalfield	Grab sample	Siltstone

Table 2
Effect of different heating conditions on muffle furnace oxidation of selected coal samples

Coal sample	Weight loss after heating for 50 h at 350 °C (%)	Weight loss after heating for 60 h at 250 °C (%)	Weight loss after heating for 70 h at 150 °C (%)
LU-1	63.00	6.93	4.90
LU-24	91.92	46.34	2.86

sections of the coal seams have been devolatilised, and are rendered inapt for mining purposes (Smith and Whittaker, 1986b).

3. Sampling and analytical techniques

A series of coal samples and samples of associated non-coal strata were obtained from both coalfields; information in the stratigraphy, location and rock type for these samples is given in Table 1.

Excessive amounts of organic matter tend to obscure mineralogical analysis in various ways, and make detection of minerals in low concentrations difficult. A key objective of the experiments for the present study was to separate the mineral matter from the organic matter, to avoid interference caused by the organic fraction when focussing only on the mineral matter. Several different methods were tested for mineral matter evaluation, partly in an attempt to develop low-cost techniques using simple equipment, and partly to evaluate more fully the nature of the mineral matter.

Representative portions of selected coal samples were placed in porcelain holders, and heated in a muffle furnace under three different conditions: 50 h at 350 °C, 60 h at 250 °C, and 70 h at 150 °C. According to Kruger (1981) an ashing temperature of 350 °C is optimum; ashing at higher temperatures may result in changes to the mineralogical composition, whereas the ashing process is significantly slower at lower temperatures. The weight loss associated with each experiment (i.e. the proportion of organic matter oxidised under each set of conditions) is summarised in Table 2, illustrating the effectiveness of ashing at 350 °C, compared to the lower temperatures.

Most of the minerals reported in coal would not be expected to undergo significant transformations at temperatures up to 350 °C (Ribbe, 1974; Vaughan and Craig, 1978; Kruger, 1981; Reeder, 1983; Nriagu and Moore, 1984). However, the results obtained from the present study show that ashing in a muffle furnace can bring about phase changes, depending on the conditions used for the procedure and the mineral assemblage involved. The X-ray diffraction patterns of two samples after heating the coal to different temperatures are illustrated in Figs. 3 and 4.

In Fig. 3 the pattern after heating remains similar to that of the relevant raw coal, despite heating to progressively higher temperatures. The background

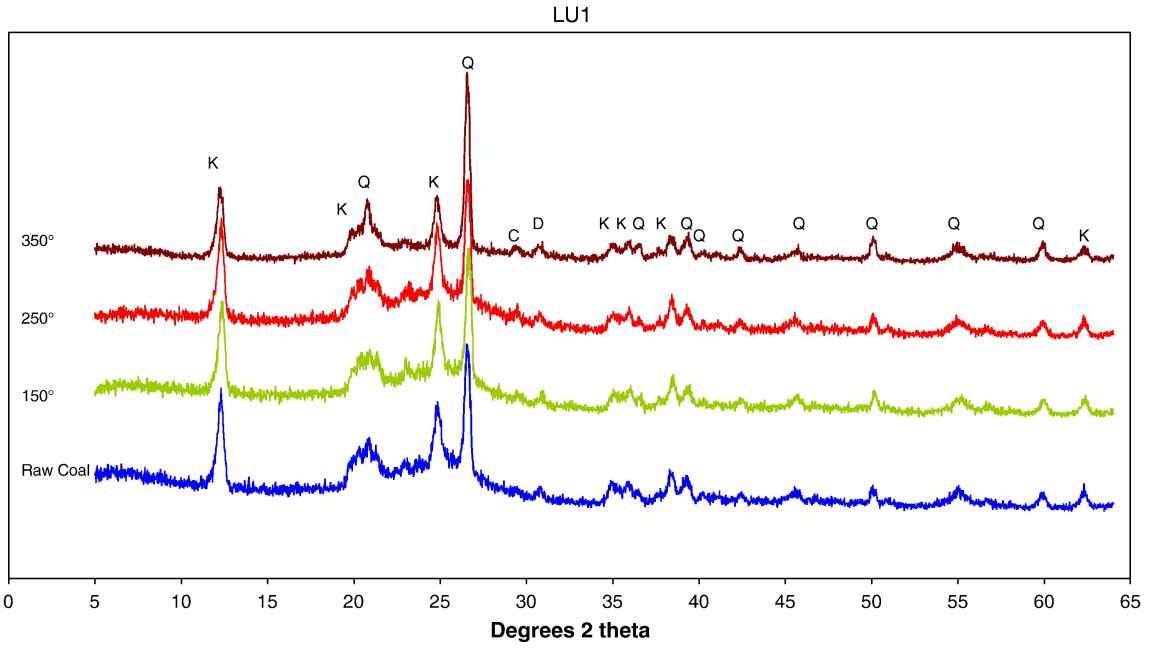

Fig. 3. X-ray diffraction scans of coal sample LU1 heated to different temperatures. Q = quartz, K = kaolinite, C = calcite, D = dolomite.

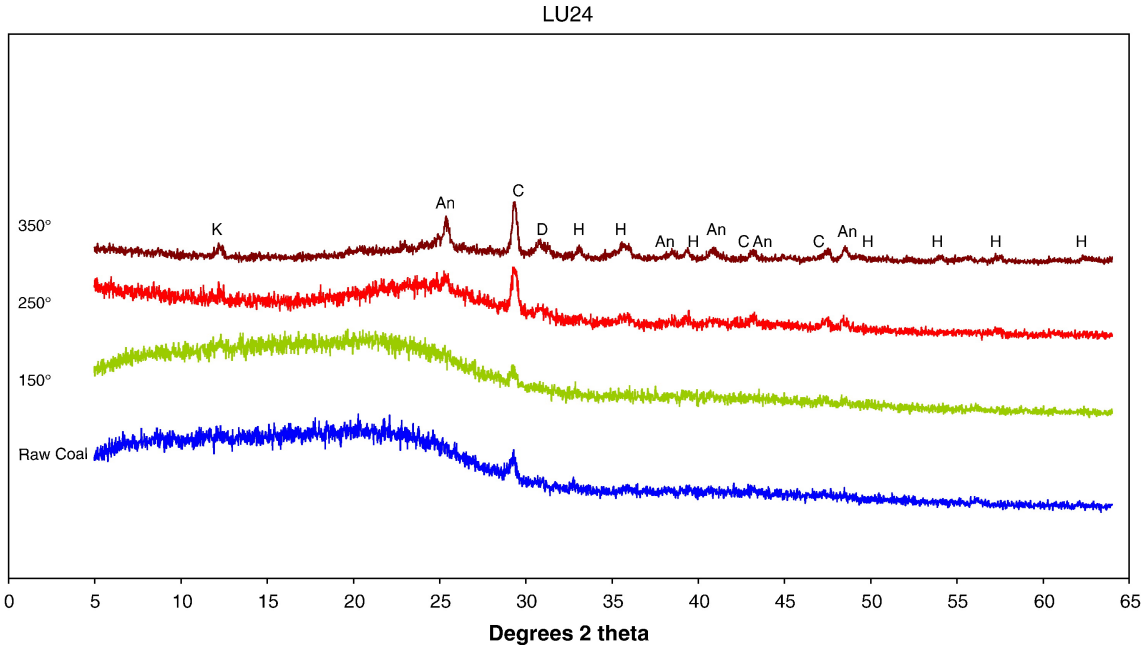

Fig. 4. X-ray diffraction scans of coal sample LU24 heated to different temperatures. K = kaolinite, C = calcite, D = dolomite, An = anhydrite, H = hematite.

due to unoxidised organic matter in this particular sample is also subtle, and the strongest peaks of calcite and dolomite can be recognised, even in the XRD trace of the raw coal sample. The XRD pattern and the low percentage weight loss at 350 °C (63%, i.e. 37% ash) both suggest that there is a significant proportion of crystalline inorganic matter present in this sample. Most of the minor mineral phases appear to be detectable by XRD of the raw coal, even though more than half of the material in the raw coal is made up of organic material that is burned off at 350 °C.

A larger proportion of organic material was removed by heating of the sample illustrated in Fig. 4 (i.e. the sample has a low overall ash yield), but the mineral phases remaining in the ash also appear to have undergone alteration with heating, especially at 350 °C. The peaks on the diffraction patterns are more visible in the samples ashed at progressively higher temperatures, due to removal of the organic matter. In the ash produced at 350 °C the peaks due to the various mineral phases are prominent. However, the minerals identified by X-ray diffraction of the ashed coal are not necessarily those present in the original coal sample, due to reactions that appear to have taken place in the furnace during heating.

Peaks due to calcite in Fig. 4 are prominent in the raw coal and in the coal after heating to all of the temperatures studied. However, kaolinite, anhydrite, dolomite, and hematite only appear in the material heated at 350 °C. Although not recognised in the unheated sample, kaolinite is the dominant clay mineral in most South African coals (Gaigher, 1980), and would therefore be expected to be present even in the raw coal material. Anhydrite and hematite, however, which are identified in the ash produced at 350 °C, have not been observed in South African coals by Gaigher (1980), Azzie (2002) or Bühmann and Bühmann (1988), and thus their occurrence in the heated samples in the present study could represent an alternative mode of origin.

The hematite, for example, probably reflects oxidation of pyrite in the coal, as indicated by Ward et al. (2001a) from similar studies of a range of American coal samples. The anhydrite ($CaSO_4$) was probably formed by interaction of organically associated Ca in the macerals, or Ca in solution in the pore water, with SO_2 released from either the oxidising pyrite or from organic sulphur in the decomposing maceral components. Calcite, which is present in the raw coal and could also have supplied Ca for anhydrite formation, would not be expected to decompose to CaO and CO_2 until much higher temperatures were reached. Indeed, as indicated above, peaks due to calcite are still present in the ash produced from this sample after heating to 350 °C.

Low-temperature oxygen-plasma ashing is an established method of isolating mineral matter and is described thoroughly by Gluskoter (1965). Oxygen is

passed through a high-energy electromagnetic field produced by a radio-frequency oscillator. An electrodeless ring discharge takes place in the gas and activated oxygen is produced, representing a mixture of atomic and ionic species in vibrationally excited states. The activated oxygen passes over the coal sample, which is placed in a Pyrex boat 5 cm below the radio-frequency field until the organic matter is decomposed. The actual ashing temperature appears to lie between 150° and 200 °C. A light-coloured dry mineral residue remains when the oxidation process is complete (Gluskoter, 1965; Ward, 1986). This technique probably represents the most reliable method for determining the percentage of total mineral matter in coal (Ward, 1999, 2002).

Ten coal samples (Table 1) were ashed in an IPC (International Plasma Corporation) low-temperature asher at the University of New South Wales, and the resulting LTA analysed using X-ray diffraction combined with the interactive, Rietveld-based Siroquant™ interpretation software (Taylor, 1991; Ward et al., 2001a). The results are indicated in Table 3. Fig. 5 illustrates the difference in peak visibility before and after one of these samples was subjected to the low-temperature ashing process. Peaks due to the dominant minerals, quartz, kaolinite and pyrite, are visible in the XRD pattern obtained from the raw coal of this sample (upper scan), but are obscured by a high background caused by the abundant organic material also present. After low-temperature ashing, however, the peaks are much readily differentiated from the background (lower scan), and more readily analysed than those in the raw coal pattern.

Three reference coals from South African sources, widely used as certified reference materials for major and trace element studies (Ring and Hansen, 1984), were also subjected to low-temperature ashing, XRD and Siroquant analysis (Table 4). These were intended to provide a basis for checking the mineralogical and chemical data against recognised international standards, as well as to widen the database on mineral matter in South African coals.

A series of rock samples from the roof and floor lithologies located in the vicinity of the coal samples (Table 1) was also analysed using XRD and Siroquant, without the need for a preliminary low-temperature ashing process. A typical XRD pattern is illustrated in Fig. 6. The Siroquant results for the rock samples are given in Table 5.

The coal samples were ashed in air at 815 °C, and the resultant ash was calcined at 1050 °C and then fused into a borosilicate disk for analysis by X-ray fluorescence (XRF) spectrometry at the University of New South Wales (UNSW) following the method described by Norrish and Chappell (1977). Chemical analysis of the coal ash, and also the ash yield at 815 °C, is given in Table 6. The ash yields at 815 °C are slightly but consistently lower than the LTA percentages of the corresponding coals as determined by oxygen-plasma ashing (Fig. 7), due to breakdown of mineral structures that occur at the higher temperatures involved. Linear regression analysis from the resulting plot (see correlation equation in Fig. 7) suggests that, for the coals studied, the proportion of LTA or mineral matter is typically about 1.3 times that of the conventional (815 °C) ash yield. This factor may be of significance in expressing analysis of coals from the study area to a mineral matter free basis in cases where more direct data on the mineral matter or LTA percentage are not available.

The chemical composition of the mineral mixtures in the LTA of each of the coal samples, including those of the international reference materials, was evaluated from the respective mineral percentages and mineral compositions, following the procedure described by Ward et al. (1999, 2001a). The percentages of the relevant oxides inferred from the mineralogical analyses were then plotted against the actual percentages of the same oxides as determined by XRF analysis of the coal ash (Fig. 8), expressed to a SO_3-free basis. In the case of the

Table 3
Mineralogy of LTA from coal samples (wt.%) based on XRD and Siroquant

Sample	LTA	Quartz	Kaolinite	Illite	I/S	Calcite	Dolomite	Siderite	Pyrite	Apatite	Goyazite	Bassanite	Jarosite	Alunite
BH 1-5	26.5	1.7	39.9	6.1	24.1	7.2	16.5	0.7	1.4		1.1			
DOU-37	25.0	27.5	66.4		5.2		0.4					0.5		
KHU 10-2	28.1	0.6	73.2	2.5		6.7	14.7		1.1			1.3		
KOR-10	32.3	0.2	78.4	4.6		3.7	10.3		1.6			1.3		
LK-1	22.3	7.4	28.8	3.7		2.8	15.5	16.1	23.1			2.7		
LU-13	13.3	22.7	59.5	1.4	8.3	1.4	2.2					4.6		
M-20	31.5	21.5	51.5	12.2	3.9				11.0					
OPT-12	19.0	22.0	73.4	4.4					0.2					
R2-M	29.5	9.1	68.2	4.7		2.6	5.1	0.3		5.4	2.6	1.8		
DEL-4	36.5	0.7	18.9	1.7		15.1			54.9	3.9	0.9	0.7	0.9	2.3

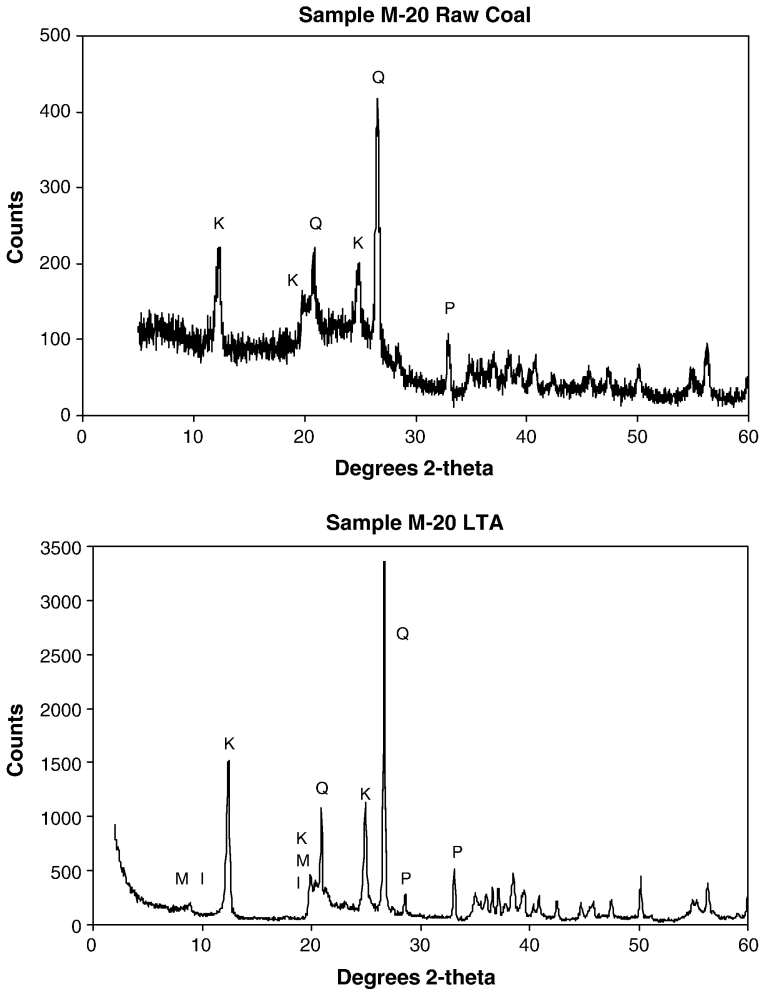

Fig. 5. X-ray diffractograms of whole-coal (top) and LTA (bottom) coal sample (M-20) with 31.5% mineral matter. Q = quartz, K = kaolinite, I = illite, M = mixed-layer illite/smectite, P = pyrite.

reference materials, the certified values provided with the samples were used, converted to represent the equivalent of SO_3-free ash analysis data. Linear regression lines are shown for each plot, together with the equation for each regression line ($y=ax+b$) and the relevant correlation coefficient (R^2) for the main series of coal samples. A diagonal line is also drawn on each graph, representing the line along which the points would fall if the proportions of the relevant oxide estimated from the Siroquant data were exactly equal to those determined directly by chemical analysis. For a perfect correlation, all points would plot along this line, and the correlation equation parameters would be: $a=1$, $b=0$, and $R^2=1.0$.

Strong correlations were obtained for SiO_2, Al_2O_3, Fe_2O_3, CaO and MgO, with high R^2 values, low values for b, and with values for a close to 1. Since these components make up the bulk of the inorganic elements

Table 4
Mineralogy of South African reference coal samples (wt.%), based on XRD and Siroquant

Sample	LTA	Quartz	Kaolinite	Illite	I/S	Calcite	Dolomite	Siderite	Pyrite	Anatase	Analcite	Bassanite	Jarosite	Coquimbite
SARM-18	11.3	28.3	34.1		31.0		0.8	0.3		0.5		4.2		0.7
SARM-19	35.2	15.5	36.3		29.6	0.7			5.3	1.5	1.5	9.6		
SARM-20	49.8	14.5	68.7			1.5	1.7	2.6	2.0	1.3		7.8		

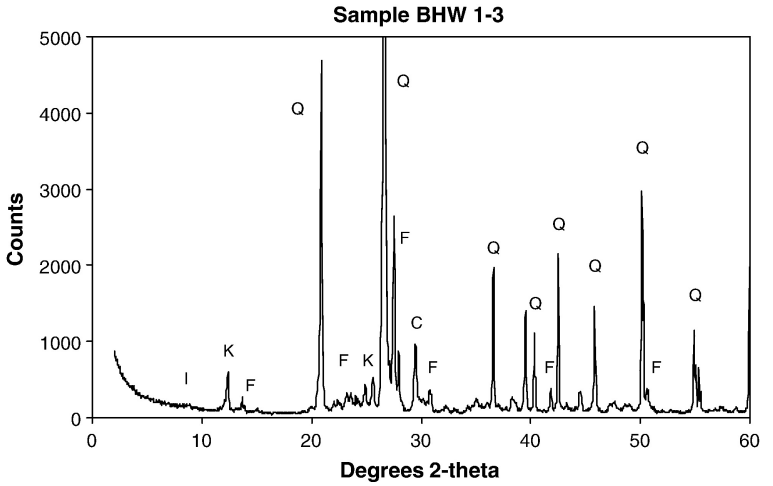

Fig. 6. X-ray diffractogram of a non-coal rock sample (BHW 1-3). Q = quartz, F = feldspar (microcline and anorthite), I = illite, K = kaolinite, C = calcite.

identified in the ash samples, the Siroquant data would appear to be consistent with the chemical analysis results.

The plot for K_2O, however, suggests that Siroquant may have overestimated the proportion of potassium-bearing minerals compared to the XRF data. This probably reflects differences between the potassium content of the illite and illite/smectite used in developing the inferred chemical composition from the Siroquant data and the actual chemistry of these particular clay mineral components. The inferred data were based on the assumption that the exchange positions in the illite lattices in each case were fully saturated with potassium, whereas the K_2O content of the illite in the actual coals may be somewhat less, due to ion exchange and/or degradation processes.

The coal samples were also analysed at UFS for major and trace elements using whole-coal XRF techniques. Although less widely used for major element analysis than the fused-disk technique, whole-coal XRF analysis avoids the possible effect of any changes in chemical composition as associated with ashing and fusing the samples in borosilicate disk preparation. Pressed powder briquettes were made for the whole-coal XRF analysis by combining 32 g of each powdered coal sample with 8 g of Hoechst Wax C, with the combination being intimately mixed for 30 min in a Turbula mixer in each case. This mixture was then pressed at 15 t pressure into 40 mm diameter cylindrical briquettes, which were used for both major and trace element analysis of coal samples. The results for the whole-coal XRF analysis are given in Tables 7 and 8.

Total sulphur in the coal samples was also determined in analysing the briquettes by XRF techniques. The results differ in many cases from the fused-disk XRF data (Table 6), since a significant part of the sulphur is typically lost during the ashing process. The whole-coal XRF results were also normalised to a loss

Table 5
Mineralogy of rock samples (wt.%) based on XRD and Siroquant

Sample	Lith'gy	Quartz	Kaolinite	Illite	I/S	Chlorite	Calcite	Dolomite	Siderite	Pyrite	Microcline	Albite	Anorthite	Rutile
BHW 1-3	Ss	60.0	7.1	2.4			1.9				20.9		6.4	1.3
DOU-35	Slst	39.1	33.3	3.9	2.3			2.4	1.2	9.1	7.0	0.2	0.6	1.0
DOU-39	Ss	51.8	41.2	2.8			1.1	2.0	0.1					1.0
M-21	Slst	61.4	17.0	4.2	3.4						12.9			0.9
M-22	Ss	30.0	38.1	9.9	4.3				0.4	2.3	13.0		0.4	1.7
OPT-3	Ss	58.3	19.1	0.6	0.7						17.3		2.7	1.4
OPT-11	Ss	80.5	7.6		1.2					0.6	10.1			
R2RO	Slst	29.8	43.7	16.1		4.8			0.4		4.7			0.5
R4FLG	Ss	74.2	18.1					0.2	6.7					0.7
R4PT	Slst	33.8	48.0	11.3							5.3		1.3	0.4

Table 6
Chemical composition of ash prepared at 815 °C from coal samples (wt.%), determined by fused-disk XRF analysis

Sample	Ash	SiO_2	TiO_2	Al_2O_3	Fe_2O_3	MgO	CaO	Na_2O	K_2O	P_2O_5	SO_3	LOI	Total
BH 1-5	20.0	38.15	1.204	29.12	2.65	4.08	11.62	1.32	1.079	0.689	7.665	2.53	100.11
DOU-37	22.1	62.68	1.512	30.52	0.36	0.52	1.53	0.37	0.359	0.082	1.246	0.75	99.93
KHU 10-2	22.3	37.45	1.808	33.42	3.44	3.48	10.06	0.17	0.343	0.324	6.857	1	98.35
KOR-10	26.6	42.32	1.806	37.01	2.79	2.06	6.5	0.27	0.384	0.192	5.19	1.9	100.42
LK-1	18.1	24.92	0.647	14.46	29.19	3.59	11.22	0.44	0.168	0.061	12.27	3.65	100.62
LU-13	10.7	56.26	1.149	29.97	0.87	1.36	4.56	0.36	0.508	0.042	3.15	1.06	99.29
M-20	24.8	57.78	1.122	27.21	9.65	0.38	0.27	0.2	1.195	0.08	0.095	0.75	98.73
OPT-12	15.2	58.9	2.686	32.04	0.8	0.36	0.35	0.46	0.56	0.229	0.32	1.13	97.84
R2-M	23.4	48.68	1.423	32.15	1.51	1.2	8.6	0.25	0.469	4.59	3.85	2.08	104.80
DEL-4	25.5	10.54	0.604	10.29	57.05	0.64	9.96	0.48	0.429	1.125	7.519	0.62	99.257
SARM-18		56.19	1.03	23.29	2.63	1.00	1.63	0.16	1.31	0.06	12.69		100.00
SARM-19		48.42	1.10	25.86	5.65	0.65	4.49	0.94	0.77	0.10	12.03		100.00
SARM-20		50.67	1.81	32.33	3.36	1.23	5.37	0.77	0.40	0.40	3.66		100.00

on ignition-, H_2O- and S-free basis (Table 8), to allow more consistent comparison of the data obtained from the different techniques.

A strong overall correlation was also noted between the inferred chemistry from the Siroquant data and a separate series of fused-disk XRF analyses carried out at UFS on the set of rock samples included in the study (Table 9; Fig. 9). Correlation coefficients for SiO_2, Al_2O_3, Fe_2O_3, and K_2O are above 0.85, and the plots are close to the 'equality line'. Differences were noted between the XRD data and the observed chemistry for CaO and MgO, but these may be due to the presence of fine-grained or amorphous carbonate in the rock samples, which was not detected by the XRD analysis.

4. Mineral abundance in coal and non-coal strata

As indicated in Table 2, the coals studied have mineral matter contents (LTA yields) of between 13 and 36%, with most of the samples having between 20 and 30% mineral matter. Quartz forms only a minor proportion of the mineral matter, typically making up either less than 10% or between 20 and 30% of the LTA residues. The non-coal rocks have significantly higher quartz contents (Table 4), with XRD analysis indicating between 30 and 60% quartz for the siltstones and up to 90% quartz for the sandstones. Most of the non-coal rocks also contain significant proportions (5 to about 25%) of feldspar, chiefly in the form of microcline. Feldspar is not present in the LTA of the coal samples, however, suggesting that the feldspar is a detrital constituent that did not penetrate with other sediments into the original peat swamp or, if it did penetrate, was destroyed by chemical reactions in the swamp environment.

Kaolinite is the dominant clay mineral in both the coals and the non-coal strata. It is more abundant in the coals (20–80% of the LTA) than in the non-coal strata (7–48%). The difference is even more marked if allowance is made for the dilution effects of the pyrite and carbonate minerals that are also present (see below) in some of the coal samples (Table 2). The other clay minerals are illite and interstratified illite/smectite, which, although abundant in one LTA sample from the Highveld field (BH-1 in Table 2), typically make up in total less than 15% of the mineral assemblage in both the coals and the non-coal materials. A trace of chlorite is also noted in one of the siltstone samples (R2RO in Table 4).

Considerable proportions of pyrite are present in some of the coal samples, with more than 50% of the LTA for one coal (DEL-4 in Table 2), and 11 to 23% for two others, being represented by pyrite in the Siroquant data. Traces of jarosite and alunite were also identified in the LTA of the most pyritic coal, possibly developed by oxidation of some of the pyrite with sample exposure or storage. The XRD study, on the other hand, shows that pyrite is in relatively low concentrations, typically up to a little more than 1%, in the LTA of most of the

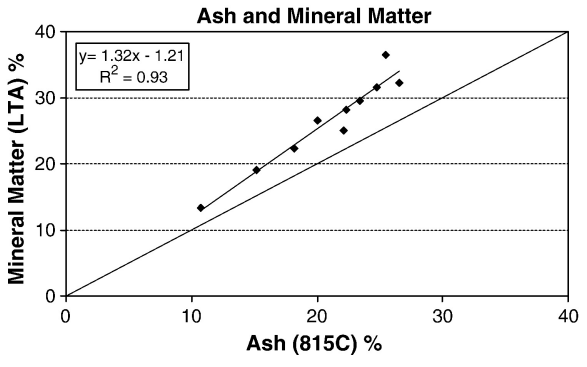

Fig. 7. Comparison of mineral matter (LTA) percentage to percentage of ash produced at 815 °C; 1:1 line also shown.

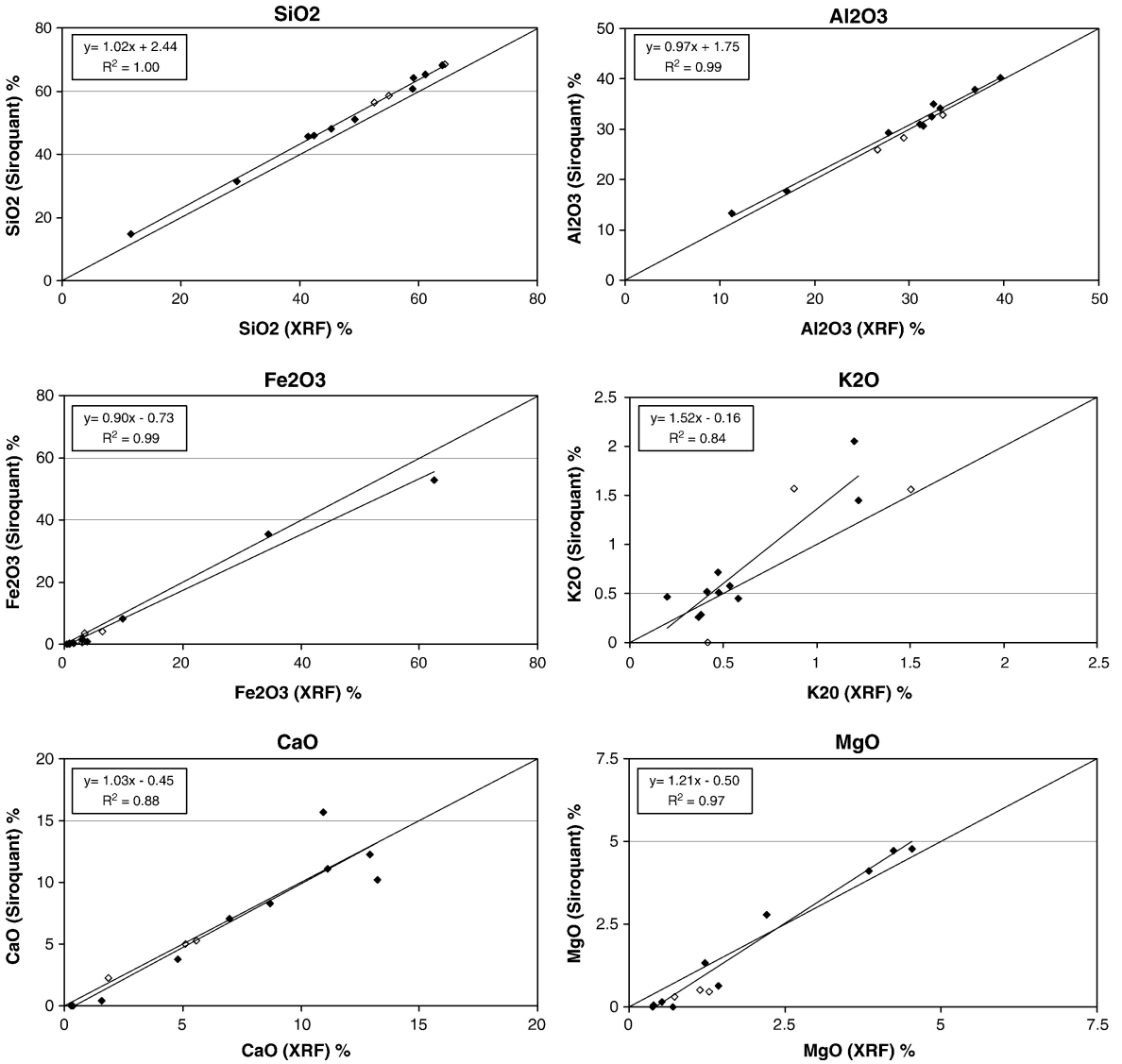

Fig. 8. Correlations between proportions of major element oxides in coal ash, measured directly by XRF analysis of ash from coals heated to 815 °C, and chemistry of coal ash inferred from mineralogy of the same coal's LTA obtained using XRD and Siroquant. Solid symbols represent coals sampled for the present study; open symbols represent certified reference materials. Equations of relevant correlation lines and correlation coefficients, obtained from linear regression analysis, are also shown in each case; 1:1 line also shown.

coal samples studied. Significant proportions of pyrite were also identified in two of the non-coal rock samples (Table 4), but most of the non-coal rocks were again identified as having no more than traces of pyrite from the XRD data.

A range of carbonate minerals is also present in the LTA of the coal samples, including calcite, dolomite and siderite. Dolomite is the most abundant of the carbonate components (Table 2), but significant proportions (up to 15%) of calcite or siderite are also present in some of the LTA residues. The carbonates are typically visible as cleat and fracture infillings in hand specimens and mine exposures, and are probably mainly of epigenetic origin. They are much less abundant in the non-coal rocks associated with the coal seams (Table 4).

Minor minerals identified in the LTA of some coal samples (Table 2) include the phosphate minerals apatite and goyazite. These occur in samples that were also found from XRF analysis to have significantly higher P_2O_5 concentrations than the other coals tested (Table 6). Traces of rutile (TiO_2) were also identified from the XRD data on the non-coal rocks (Table 4).

Table 7
XRF data (University of the Free State) — whole-coal analyses

Sample	SiO_2	TiO_2	Al_2O_3	Fe_2O_3	MgO	CaO	Na_2O	K_2O	P_2O_5	S	H_2O^-	LOI	Total
BH 1-5	6.30	0.31	4.78	0.25	0.39	2.34	0.25	0.35	0.31	0.80	3.06	82.66	101.80
DOU-37	7.99	0.27	3.91	0.12	0.09	1.25	0.00	0.07	0.00	0.63	1.25	84.67	100.25
KHU 10-2	4.73	0.44	5.12	0.71	0.63	3.95	0.00	0.07	0.07	0.67	3.29	78.36	98.04
KOR-10	7.48	0.55	6.63	0.28	0.34	1.93	0.02	0.11	0.07	0.38	2.49	81.43	101.71
LK-1	2.11	0.08	2.17	7.51	0.40	3.25	0.04	0.00	0.00	1.44	3.30	78.76	99.06
LU-13	4.32	0.14	2.76	0.08	0.04	0.67	0.01	0.07	0.00	0.55	3.64	87.31	99.59
M-20	7.59	0.21	3.19	4.68	0.00	0.00	0.00	0.23	0.01	2.89	0.95	80.30	100.05
OPT-12	11.01	0.78	4.51	0.15	0.00	0.00	0.00	0.08	0.04	0.62	3.11	79.61	99.91
R2-M	7.35	0.33	5.92	0.36	0.07	1.87	0.00	0.10	1.40	0.40	2.47	78.05	98.32

Small but significant proportions of bassanite ($CaSO_4 \cdot 1/2H2O$) were identified in most of the LTAs from the coal samples (Table 2). As indicated in the discussion on anhydrite in the heated coals above, this material probably represents an artefact of the low-temperature ashing process, derived from the interaction of organically associated Ca with organic S during breakdown of the organic matter (cf. Ward et al., 2001a; Ward, 2002).

The minerals in the South African reference coals (SARM series, Table 3) are similar in nature, and in many cases proportional, to the minerals in the coals of the main sample suite. All three coals have relatively low quartz contents (14–28% of the LTA), abundant kaolinite, and relatively low concentrations of carbonate minerals. The LTA of sample SARM 18, from the Witbank area, and that of SARM 19 (Orange Free State) both have relatively high proportions of interstratified illite/smectite (similar to sample BH-15 in Table 2); SARM 20 (Sasolburg) has a clay mineral assemblage consisting almost entirely of the kaolinite component. The LTA of SARM 18 has no detectable pyrite, but the LTA of SARM 19 contains around 5% pyrite and that of SARM 20, with a higher LTA yield, around 2%. The LTA of SARM 20 also contains a higher proportion of carbonate minerals than the other reference coal samples. All of the reference coals also have significant proportions of bassanite in their LTA residues, suggesting that at least some of the Ca in these coals occurs in organic combination within the maceral components.

5. Influence of minerals on groundwater chemistry

Application of acid–base accounting procedures has made it possible to quantify the potential of a particular rock or coal sample to produce acidic or alkaline waters under mine drainage conditions. A detailed explanation of the experimental procedure followed in applying this technique to the present study can be found in Hodgson and Krantz (1998), Cruywagen (2000), and Usher et al. (2001). The method involves adding 120 or 80 ml of H_2O_2 reagent to 1 to 4 g of a pulverised sample and allowing it to effervesce. The final pH is measured once effervescence has ceased. The supernatant liquid is then analysed for sulphate. The % S (total) can also be determined by a Leco elemental analyser if required.

The actual acid produced during the oxidation of pyrite by H_2O_2 is termed potential acidity. The reaction, which represents the complete oxidation of Fe^{2+} and S_2^{2-}, is as follows:

$$FeS_2 + 7.5H_2O_2 = Fe(OH)_3(s) + 2H_2SO_4 + 4H_2O$$

This reaction demonstrates that the complete oxidation of pyrite liberates 2 mol of H_2SO_4 for every mole of FeS_2 oxidised (Cruywagen, 2000). The neutralising potential is determined by adding 15 ml of 0.06 N

Table 8
XRF data (University of the Free State) — whole-coal analyses — normalised loss on ignition-, H_2O- and S-free

Sample	SiO_2	TiO_2	Al_2O_3	Fe_2O_3	MgO	CaO	Na_2O	K_2O	P_2O_5	Total
BH 1-5	41.23	2.03	31.28	1.64	2.55	15.31	1.64	2.29	2.03	100.00
DOU-37	58.32	1.97	28.54	0.88	0.66	9.12	0.00	0.51	0.00	100.00
KHU 10-2	30.09	2.80	32.57	4.52	4.01	25.13	0.00	0.45	0.45	100.00
KOR-10	42.96	3.16	38.08	1.61	1.95	11.09	0.11	0.63	0.40	100.00
LK-1	13.56	0.51	13.95	48.26	2.57	20.89	0.26	0.00	0.00	100.00
LU-13	53.43	1.73	34.13	0.99	0.49	8.29	0.07	0.87	0.00	100.00
M-20	47.71	1.32	20.05	29.42	0.00	0.00	0.00	1.45	0.06	100.00
OPT-12	66.45	4.71	27.22	0.91	0.00	0.00	0.00	0.48	0.24	100.00
R2-M	42.24	1.90	34.02	2.07	0.40	10.75	0.00	0.57	8.05	100.00

Table 9
Chemical composition of rock samples by fused-disk XRF techniques

Sample	SiO_2	TiO_2	Al_2O_3	Fe_2O_3	MnO	MgO	CaO	Na_2O	K_2O	P_2O_5	S	H_2O^-	LOI	Total
BHW1-3	81.00	0.38	6.08	1.53	0.02	0.00	3.10	0.74	2.77	0.03	0.44	0.15	3.74	99.98
DOU35	54.20	1.80	15.18	4.59	0.03	1.43	0.75	0.05	1.29	0.09	0.52	0.61	19.26	99.80
DOU39	47.42	1.16	10.19	1.02	0.03	0.74	2.95	0.01	0.41	0.02	0.23	0.67	34.42	99.27
M21	77.48	0.69	12.20	1.10	0.01	0.00	0.03	0.06	2.82	0.03	0.24	0.49	4.77	99.92
M22	62.16	0.90	18.73	3.00	0.02	0.43	0.11	0.04	2.81	0.06	0.45	0.73	10.99	100.43
OPT3	79.66	0.70	11.28	0.48	0.01	1.01	0.03	0.10	2.94	0.05	0.01	0.23	3.42	99.92
OPT11	89.35	0.44	4.73	1.38	0.01	0.00	0.00	0.05	0.78	0.02	0.38	0.16	2.81	100.11
R2RO	53.64	1.06	22.35	2.01	0.01	0.56	0.37	0.54	1.61	0.10	0.14	1.10	15.95	99.44
R4FLG	75.43	3.84	5.03	6.10	0.20	0.50	0.35	1.55	0.25	0.03	0.34	0.20	6.38	100.20
R4PT	53.74	0.95	23.10	0.58	0.01	0.29	0.17	0.61	1.25	0.04	0.26	0.99	17.23	99.22

standardised H_2SO_4 to 5 g of a pulverised sample. The pH of the mixture must be below 2.5 after 24 h before back titration to a pH of 7 is carried out with 0.06 N NaOH. If the pH is still above 3 after 24 h, additional acid is added and the process is repeated until the correct pH is obtained (Usher et al., 2001).

The solubility of calcite is different for open and closed systems, and thus the acid and neutralising potential for both cases was determined. In an open system carbon dioxide dissolves into the atmosphere. Therefore, 1 mol of FeS_2 is neutralised by 2 mol of $CaCO_3$. In a closed system carbon dioxide is dissolved in the water and carbonic acid or H_2CO_3, is formed. It follows that the required $CaCO_3$ needed to neutralise 1 mol of FeS_2 is 4 mol (Cruywagen, 2000).

The acid potential (AP) is a measure of the potential of a sample to generate acidity. The amount of calcite required to neutralise a given amount of acid mine drainage depends on the behaviour of CO_2 during neutralisation and on the pH reached. If the AMD is to be neutralised to pH 6.3 or above, then the following reaction may be written:

$$FeS_2 + 2CaCO_3 + 3.75O_2 + 1.5H_2O = Fe(OH)_3 + 2SO_4^{2-} + 2Ca^{2+} + 2CO_2$$

For each mole of pyrite that is oxidised, two moles of calcite are required for acid neutralisation. On a mass ratio basis, for each gram of sulphur present, 3.125 g of calcite is required for acid neutralisation. When expressed in parts per thousand of spoil, for each 10 ppt of sulphur present 31.25 ppt of calcite is required for acid neutralisation. The stoichiometry in the previous equation is based on the exsolving of carbon dioxide gas out of the spoil system. In a closed system, carbon dioxide is not exsolved, and additional acidity from carbonic acid is generated. Cravotta et al. (1990) proposed that up to 4 mol of calcite might be needed for acid neutralisation. Twice as much calcite would be required for acid neutralisation in a closed system, compared to an open system. On a mass basis, for each 10 ppt of sulphur present, 62.5 t of calcite is needed for acid neutralisation in one thousand tons of spoil (Cravotta et al., 1990).

Results obtained from the laboratory experimental procedure are used in calculating the AP, neutralising potential (NP) and net neutralising potential (NNP) as follows:

$$\mathrm{AP} = \frac{SO_4(\mathrm{mg/L})/\mathrm{weight(g)}}{1000} \times \mathrm{ml\ H_2O\ or\ H_2O_2} = \mathrm{kg\ SO_4/t\ of\ sample}$$

$$\mathrm{AP(Open)(CaCO_3 kg/t)} = \frac{SO_4\mathrm{kg/t}}{48} \times 50$$

$$\mathrm{NP(CaCO_3 kg/t)} = (\mathrm{N\ H_2SO_4} \times \mathrm{ml\ acid}) - (\mathrm{N\ NaOH} \times \mathrm{ml\ alkali})/\mathrm{weight(g)} \times 50$$

Thus, the NNP is determined by subtracting the acid potential from the neutralising potential.

$$\mathrm{NNP(Open)} = \mathrm{NP} - \mathrm{AP(Open)}$$

In a closed system, AP (Closed)=AP (Open)×2, and, NNP (Closed)=NP−AP (Closed) (Hodgson and Krantz, 1998).

There are various types of screening criteria used to interpret acid–base accounting results. In this study the NNP was used as a screening criterion. Research has shown that there is a range from −20 to 20 kg/t $CaCO_3$ where a sample can become acidic or remain neutral. Thus, a sample with a NNP <20 is potentially acid generating and a sample with a NNP >20 might not generate acid (Usher et al., 2001).

5.1. Application to the Witbank Coalfield

Acid–base data from 64 rock and coal samples were available for the Witbank Coalfield. The data were

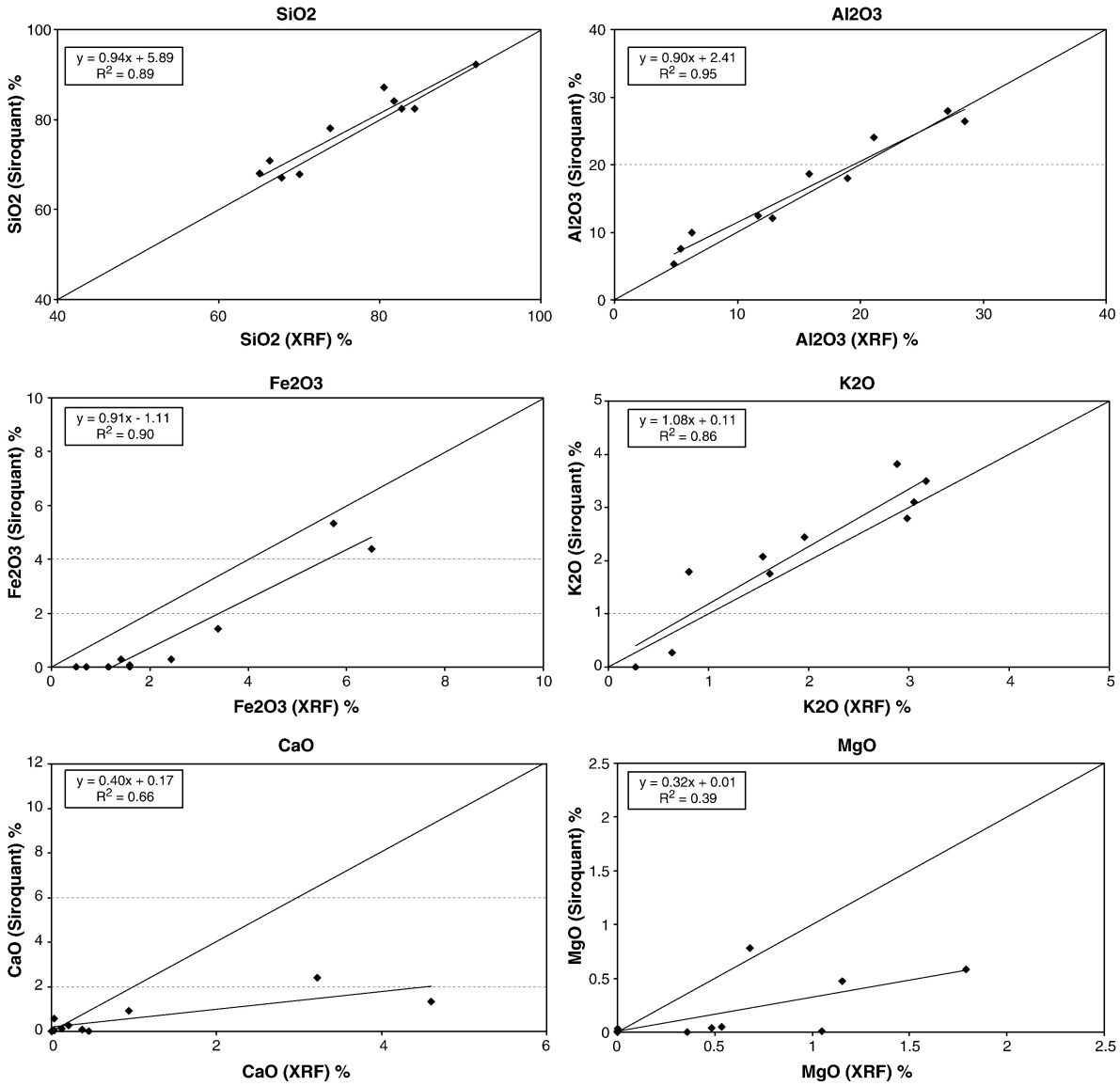

Fig. 9. Correlations between proportions of major element oxides in non-coal rock samples, measured directly by XRF analysis, and chemistry inferred from the mineralogy of the same samples obtained using XRD and Siroquant. Equations of relevant correlation lines and correlation coefficients, obtained from linear regression analysis, are also shown in each case; 1:1 line also shown.

organised according to lithologies, ranging from below the No. 1 seam at the bottom of the dataset to above the No. 5 seam at the top. Average values were used to illustrate the vertical distribution of acid and neutralising potentials in the coalfield. Fig. 10 shows that the natural or initial pH of both rock and coal samples are close to alkaline or at least to neutral conditions. A possible reason for the initial pH of the No. 5 seam being much lower could be because it is situated closer to the water table. The final pH of all lithologies indicates that acidic conditions would dominate if complete sulphide oxidation were to occur. The No. 5 seam also has a lower final pH, suggesting that total available carbonates could already be leached out leaving a lesser source of alkalinity to buffer the acid. It could also be that acid-producing constituents were originally more abundant than acid consuming constituents.

Fig. 11 shows that the acid potential for both open and closed systems exceeds the neutralising potential by excessive quantities. Only between the No. 1 and No. 2 seams would sufficient alkalinity be provided to buffer acidity. CaO and MgO concentrations are not high enough in the roof rocks of the No.1 seam and the floor rocks of No.2 seam to clarify this neutralising potential

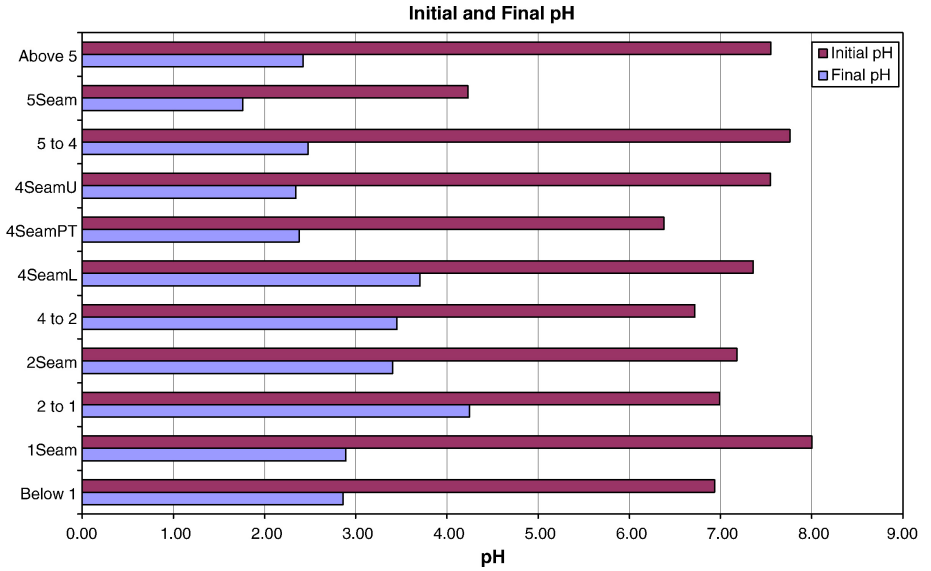

Fig. 10. Initial and final pH of the samples before and after complete pyrite oxidation and carbonate dissolution, Witbank Coalfield.

completely. The presence of feldspars and other aluminosilicates would contribute to the neutralising potential even if weathering occurs at a slow rate (Banwart and Malmström, 2001). However, actual acid and neutralisation release rates cannot be predicted with the technique, neither can the completeness of the reaction be assessed (Cruywagen, 2000).

Acid–base accounting data on these coalfields have been generated by the Institute for Groundwater Studies at the UFS, and are often presented as case studies in reports such as the Water Research Commission Reports (e.g. Hodgson and Krantz, 1998). The investigation described in the present paper was intended to confirm that the lithological units in the coal-bearing sequence will contribute greatly and negatively to the water quality in the area, unless remediation programs are implemented. A negative net neutralising potential (NNP) is shown in Fig. 12 for all lithological units

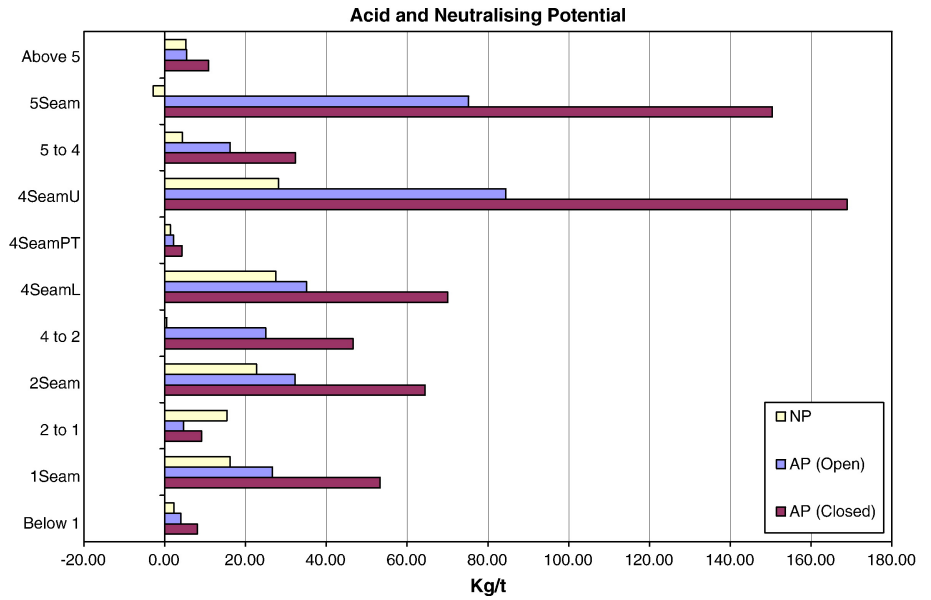

Fig. 11. Stratigraphic variation in acid potential (for an open and closed system) and neutralising potential for the Witbank Coalfield.

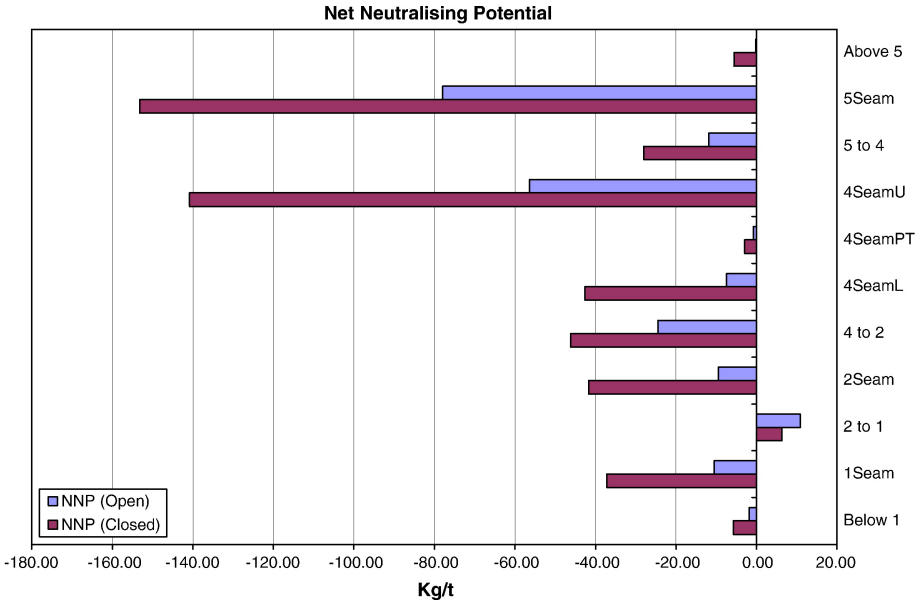

Fig. 12. Stratigraphic variation in net neutralising potential for the Witbank Coalfield.

except between the No.1 and No. 2 seams. The more negative the NNP becomes, the more $CaCO_3$ per tonne of spoil will have to be added to neutralise the acidity.

The constant decrease in the AP, NP and NNP with depth is possibly due to a lack of pyrite, invoking a lack of leaching of reactive species in the lower units; however, these trends could also be a result of diagenetic controls and/or influence of the depositional environment on the distribution of mineral matter. Although sulphur may increase or decrease in a specific direction horizontally within a seam, no exact distribution was noted vertically in individual boreholes, or for the dataset as a whole. Sulphur percentages are extremely variable, and range from 0.01 to as much as 8.0 wt.% of individual samples. A multiple regression analysis performed on these samples shows that the sulphur percentage is 95% accountable for the NNP. For most units the NNP is almost equivalent to or slightly less than the AP. A negative NNP indicates the inability of a sample to provide sufficient neutralising constituents to buffer the acid produced.

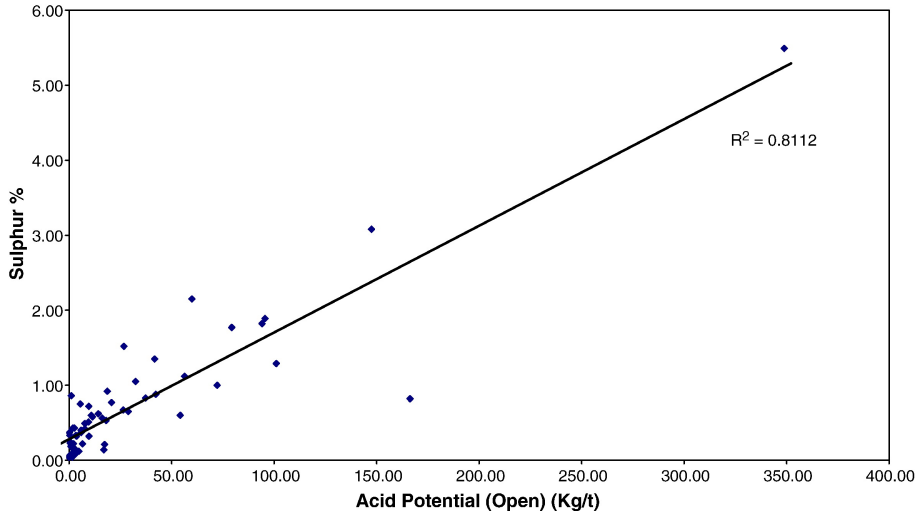

Fig. 13. Plot showing relation between acid potential (for an open system) and sulphur %, Witbank Coalfield.

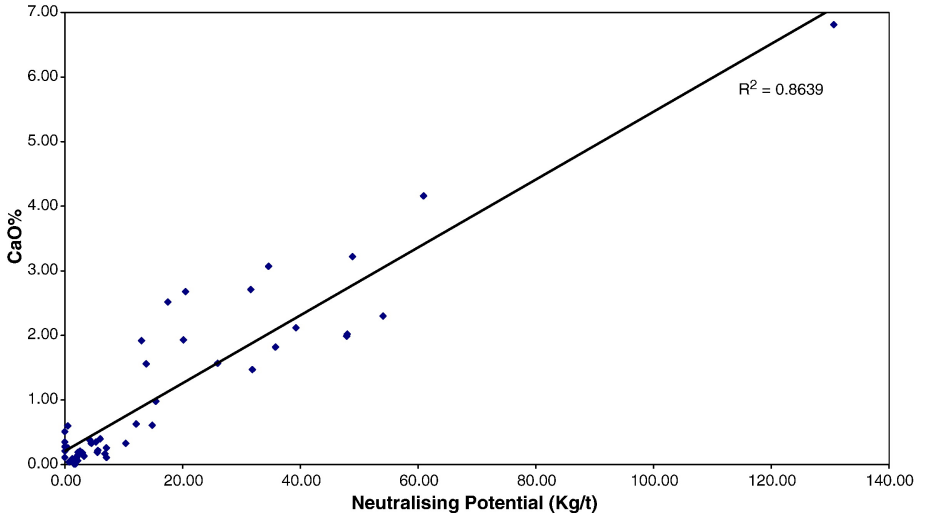

Fig. 14. Plot showing relationship between neutralising potential and CaO %, Witbank Coalfield.

Strong correlations between the AP and S %, and NP and CaO % can be seen in Figs. 13 and 14, respectively. The sulphur obtained from XRF analyses is in good agreement with the AP (closed) as seen in Fig. 13 ($r^2=0.811$). Correlations for Fe_2O_3 and AP are insignificant, possibly due to the fact that most of the Fe_2O_3 was not present as pyritic Fe_2O_3 but as $FeCO_3$ (siderite), in dolomite, or in illite or illite/smectite. A significant correlation was obtained for the NP and CaO % ($r^2=0.864$, Fig. 14) as well as the combined CaO and MgO % ($r^2=0.821$) and the NP. The percentages of S and CaO cover a similar range and have similar degrees of correlation to the AP and NP, respectively. However, the AP for a coal with a given concentration of S is almost four times more than the NP for a coal with an equivalent amount of CaO. Thus, the NNP is mainly accounted for by the S concentration.

According to the screening criteria proposed by Usher et al. (2001), the results for the units between the No. 1 and No. 2 coal seams are considered to be inconclusive. However, the average NNP values suggest that only No. 5 coal seam, No. 4 Upper coal seam, and between No. 4 and No. 2 coal seams are potentially acid generating. The other units could become either acidic or neutral.

5.2. Application in the Highveld Coalfield

Limited acid–base accounting data were available for this coalfield, yet from the data for No. 4 and No. 5 seams of the Highveld Coalfield, it seems that the same situation could be expected as in the Witbank Coalfield. Highly negative NNP values are also observed for the coal seams. Values range from approximately −156.14 to −25.66 kg/t.

The acid–base accounting method is based on ideal situations, where it is assumed that complete oxidation of sulphides and dissolution of carbonates will occur. The presence of these constituents does not necessarily guarantee their availability, which is often dependent on the minerals in which certain elements are contained, as well as geochemical factors such as pH, Eh and temperature. In addition, the method does not take rates of weathering and oxidation into account. Thus, the prediction is more relevant when ideal conditions exist. Assuming that all sulphide-S is available for oxidation and that organic sulphur is low (typically 0.4 to 0.5% in this area), then the total S analysed could be used to predict the AP for samples on which no acid–base determinations have been carried out. The correlation between the XRF S and the AP for the Witbank Coalfield (Fig. 13) suggests that there should also be a strong relationship between these components for the Highveld field. The excellent correlation between the NP and CaO, and between the NP and combined CaO and MgO for the Witbank field (Fig. 14), suggests that these chemical components are also largely responsible for the NP values in the Highveld Coalfield. On this basis it should also be possible to predict the NP by using the CaO and MgO concentrations for samples for which no AP or NP data are available.

6. Conclusions

XRF and XRD analyses were conducted on various coal and sediment samples from the Witbank and Highveld Coalfields with the aim of improving the understanding of the mineralogy and geochemistry of

these coals and coal-bearing units. Different preparation and analytical procedures were applied to determine the differences that exist between the available methods. Low-temperature ashing and X-ray diffraction carried out on some samples by the University of New South Wales accentuated the need for and practicality of integrating other techniques with XRD. X-ray diffraction on LTA isolated from the coals proved to be accurate in identifying minerals that occur as minor constituents, and is especially useful where the organic material in the coal tends to obscure interpretations from raw coal XRD. However, mineral artefacts may also be generated during the ashing process.

The distribution and abundance of reacting mineral species in the coalfields can also be used to predict the extent of acidification and neutralisation in particular areas. Although the samples included in the study were inadequate as a basis for mapping of mineral concentrations, pyrite appears to be most abundant in the western part of the Witbank Coalfield (K. Pinetown, unpublished data), and hence it could be expected that acid conditions are more likely to occur in this region. The availability of carbonates will provide buffering capacity, but it is also evident that insufficient carbonates are available for long-term neutralisation. Clay minerals and other aluminosilicates are abundant in the northern region, where lesser proportions of acid-producing species are available. These minerals, together with the carbonates, might have a greater influence on the neutralising potential in the northeastern region, where lesser proportions of acid-producing species appear to be present.

Acid–base accounting data generated from this study will assist in making plausible predictions concerning the potential of the coal and non-coal rocks in the Witbank and Highveld Coalfields to contribute to acid mine drainage. This investigation has led to a better understanding of the coals and their roof and floor lithologies in the study area, and the use of this information in future applications will be of benefit to the mining industry and the associated community.

Acknowledgements

The authors wish to thank the Water Research Commission, the Department of Geology, University of the Free State and the University of New South Wales for financial assistance and all necessary resources needed to carry out this research. Thanks are also expressed to Irene Wainwright of UNSW, for assistance with the XRF analysis, and to the referees, Sue Golding and David French, for their constructive comments.

References

Azzie, B.A. 2002. Coal mine waters in South Africa: their geochemistry, quality and classification. Ph.D Thesis, University of Cape Town, South Africa.

Banwart, S.A., Malmström, M.E., 2001. Hydrochemical modelling for preliminary assessment of minewater pollution. Journal of Geochemical Exploration 74, 73–97.

Bouška, V., 1981. Geochemistry of Coal. Elsevier Scientific Publishing Company, Amsterdam. 284 pp.

Bühmann, C., Bühmann, D., 1988. Sedimentary petrology of coal-bearing Ecca sediments. Final Project Report. University of Natal, South Africa.

Cairncross, B., 2001. An overview of the Permian (Karoo) coal deposits of southern Africa. Journal of African Earth Sciences 33, 529–562.

Catuneanu, O., Hancox, P.J., Rubidge, B.S., 1998. Reciprocal flexural behaviour and contrasting stratigraphies: a new basin development model for the Karoo retroarc foreland system, South Africa. Basin Research 10, 417–439.

Cravotta, C.A., Brady, K.B., Smith, M.W., Beam, R.L., 1990. Effectiveness of alkaline addition at surface mines in preventing or abating acid mine drainage: part 1, geochemical considerations. Final Proceedings of the 1990 Mining and Reclamation Conference and Exhibition, West Virginia University, Morgantown, pp. 221–226.

Cruywagen, L. 2000. Static geochemical methods in determining acid mine drainage. M.Sc Thesis, University of the Free State, South Africa.

Gaigher, J.L. 1980. The mineral matter in some South African coals. M.Sc Thesis, University of Pretoria, South Africa.

Gluskoter, H.J., 1965. Electronic low-temperature ashing of bituminous coal. Fuel 44, 285–291.

Hodgson, F.D.I., Krantz, R.M., 1998. Groundwater quality deterioration in the Olifants River Catchments above the Loskop Dam with specialised investigations in the Witbank Dam Sub-Catchment. Technical Report to the Water Research Commission by the Institute for Groundwater Studies. University of the Free State, South Africa.

Kruger, S.J. 1981. ‘n Mineralogiese ondersoek van die asfraksie van steenkool van die Springbokvlakte-Steenkoolveld. M.Sc Thesis, Rand Afrikaans University, South Africa.

Mackowsky, M.-Th., 1968. Mineral matter in coal. In: Murchison, D.G., Westoll, T.S. (Eds.), Coal and Coal-Bearing Strata. Oliver and Boyd, London, pp. 309–321.

McCarthy, M.D.B., Newton, R.J., Bottrell, S.H., 1998. Oxygen isotopic compositions of sulphate from coals: implications for primary sulphate sources and secondary weathering processes. Fuel 77, 677–682.

Norrish, K., Chappell, B.W., 1977. X-ray fluorescence spectrometry. In: Zussman, J. (Ed.), Physical Methods in Determinative Mineralogy. Academic Press, London, pp. 201–272.

Nriagu, J.O., Moore, P.B. (Eds.), 1984. Phosphate Minerals. Springer-Verlag, Berlin. 442 pp.

Rao, P.D., Walsh, D.E., 1999. Influence of coal deposition on phosphorous accumulation in a high latitude, northern Alaska coal seam. International Journal of Coal Geology 38, 261–284.

Reeder, R.J. (Ed.), 1983. Carbonates: Mineralogy and Chemistry. Reviews in Mineralogy, vol. 11. Mineralogical Society of America. 394 pp.

Ribbe, P.H. (Ed.), 1974. Sulphide Mineralogy. Reviews in Mineralogy, vol. 1. Mineralogical Society of America. 284 pp.

Ring, E.J., Hansen, R.G., 1984. The preparation of three South African coals for use as reference materials. Report M169. Council for Mineral Technology. 130 pp.

Smith, D.A.M., Whittaker, R.R.L.G., 1986a. The coalfields of southern Africa: an introduction. In: Anhaeusser, C.R., Maske, S. (Eds.), Mineral Deposits of Southern Africa. I. Geological Society of South Africa, pp. 1875–1878.

Smith, D.A.M., Whittaker, R.R.L.G., 1986b. The Springs-Witbank coalfield. In: Anhaeusser, C.R., Maske, S. (Eds.), Mineral Deposits of Southern Africa. I. Geological Society of South Africa, pp. 1969–1984.

Smith, R.M.H., Eriksson, P.G., Botha, W.J., 1993. A review of the stratigraphy and sedimentary environments of the Karoo-aged basins of southern Africa. Journal of African Earth Sciences 16 (1/2), 143–169.

Spiker, E.C., Pierce, B.S., Bates, A.L., Stanton, R.W., 1994. Isotopic evidence for the source of sulphur in the Upper Freeport coal bed (west-central Pennsylvania, U.S.A.). Chemical Geology 114, 115–130.

Usher, B.H., Cruywagen, L., de Necker, E., Hodgson, F.D.I., 2001. On-site and laboratory investigations spoil in opencast collieries and the development of acid–base accounting procedures. Report to the Water Research Commission by the Institute for Groundwater Studies. WRC Report University of the Orange Free State. 262 pp.

Taylor, J.C., 1991. Computer programs for standardless quantitative analysis of minerals using the full powder diffraction profile. Powder Diffraction 6, 2–9.

Vassilev, S.V., Tascon, J.M.D., 2002. Methods for characterisation of inorganic and mineral matter in coal: a critical overview. Energy and Fuels 17, 271–281.

Vaughan, D.J., Craig, J.R., 1978. Mineral Chemistry of Metal Sulphides. Cambridge University Press, Cambridge. 493 pp.

Ward, C.R. (Ed.), 1984. Coal Geology and Coal Technology. Blackwell Scientific Publications, Melbourne. 345 pp.

Ward, C.R., 1986. Review of mineral matter in coal. Australian Coal Geology 6, 87–110.

Ward, C.R., 1999. Mineral characterisation for combustion — the contribution from the geological sciences. In: Gupta, R., Wall, T.F., Baxter, L.A. (Eds.), The Impact of Mineral Impurities in Solid Fuel Combustion. Kluwer Academic / Plenum Publishers, New York, pp. 23–32.

Ward, C.R., 2002. Analysis and significance of mineral matter in coal seams. International Journal of Coal Geology 50, 135–168.

Ward, C.R., Spears, D.A., Booth, C.A., Staton, I., Gurba, L.W., 1999. Mineral matter and trace elements in coals of the Gunnedah Basin, New South Wales, Australia. International Journal of Coal Geology 40, 281–308.

Ward, C.R., Taylor, J.C., Matulis, C.E., Dale, L.S., 2001a. Quantification of mineral matter in the Argonne Premium Coals using interactive Rietveld-based X-ray diffraction. International Journal of Coal Geology 46, 67–82.

Ward, C.R., Bocking, M., Ruan, C., 2001b. Mineralogical analysis of coals as an aid to seam correlation in the Gloucester Basin, New South Wales, Australia. International Journal of Coal Geology 47, 31–49.

Williamson, I.A., 1967. Coal Mining Geology. Oxford University Press, London. 266 pp.